Thermal-Mass Trade-Off Analysis of Cu-Al Bimetallic Fins in PCM-Based Battery Thermal Management

B. Nithesh[1] and T. Srihari Vikram[1,2*]

[1] School of Mechanical Engineering, SASTRA Deemed to be University, Thanjavur – 613401, Tamilnadu, India
[2] Centre for Energy Storage & Conversion, SASTRA Deemed to be University, Thanjavur – 613401, Tamilnadu, India
*harivikram@mech.sastra.edu

Abstract. Efficient thermal management is essential for maintaining the performance, safety, and lifespan of lithium-ion batteries used in electric vehicles. Phase change material (PCM)-based battery thermal management systems are attractive due to their high latent heat storage capacity and passive operation. However, the low thermal conductivity of most PCMs restricts heat dissipation and may cause localized temperature rise within battery cells. To address this limitation, metallic fins are commonly incorporated into the PCM domain to enhance heat transfer. In this study, the thermal-mass trade-off associated with Cu-Al bimetallic fins in a PCM-based battery thermal management system is numerically investigated for a cylindrical 18650 lithium-ion cell. The system consists of four radial fins embedded within PCM, and simulations are performed under a 2C discharge condition with an external convective heat transfer coefficient of 5 W/m^2K. The influence of PCM thickness (4, 8, and 12 mm) and fin material composition (100Al, 25Cu-75Al, 50Cu-50Al, 75Cu-25Al, and 100Cu) is analysed. The results show that increasing PCM thickness improves thermal buffering but reduces the rate of PCM melting due to the larger latent heat capacity. Incorporating copper into the fins significantly enhances heat spreading and PCM activation compared with aluminium fins. Bimetallic fin configurations achieve PCM melting behaviour comparable to pure copper fins while reducing copper usage, indicating their potential for efficient and lightweight battery thermal management systems.

Keywords: Battery thermal management system, Lithium-ion battery, Phase change material, Bimetallic fins, Thermal-mass trade-off.

1 Introduction

The transportation sector is a major contributor to global energy consumption and greenhouse gas emissions, making it a key focus area in the transition toward sustainable energy systems. According to the International Energy Agency, the transport sector accounts for approximately 30% of global final energy consumption, with road transport representing the largest share of this demand [1]. The continued dependence

S. Uppapalli and D. Chakraborty (eds.), *Proceedings of the International Conference on Mechanics, Materials and Mechatronics (ICM³ 2026)*, Atlantis Highlights in Engineering 47,
https://doi.org/10.2991/978-94-6239-764-4_5

on fossil-fuel-powered vehicles has resulted in significant environmental impacts, as the sector contributes nearly 24% of global energy-related CO2 emissions, of which road transport accounts for almost three-quarters of transport emissions [1,2]. In recent years, global road transport emissions have exceeded 6 Gt of CO2 annually, largely driven by passenger cars and freight transport [2]. These concerns have increased the demand for cleaner and more energy-efficient transportation technologies. Electric vehicles (EVs) are widely recognized as a practical alternative to conventional vehicles because they offer higher energy efficiency and produce no direct tailpipe emissions. In general, electric drivetrains convert more than 70–80% of the electrical energy stored in the battery into useful mechanical power, whereas conventional gasoline engines typically utilize only about 20–30% of the fuel energy for vehicle propulsion [3]. The increasing use of EVs also supports the use of renewable electricity in the transport sector. This helps reduce dependence on fossil fuels and lowers carbon emissions. As EV adoption continues to grow, the demand for advanced battery technologies has also increased. According to the IEA Global EV Outlook 2024, global demand for EV batteries exceeded 750 GWh in 2023 and is expected to surpass 3 TWh by 2030 [4]. Despite these advantages, lithium-ion batteries are highly sensitive to operating temperature. High temperatures accelerate battery degradation, reduce performance, and increase the risk of thermal runaway. Therefore, maintaining the battery within the recommended operating temperature range is essential for ensuring safety, performance, and long service life. As a result, an efficient battery thermal management system (BTMS) has become an important part of electric vehicle design.

Following the increasing demand for reliable battery operation, many researchers have investigated passive thermal management systems (BTMS) using phase change materials (PCM). Owing to their high latent heat storage capacity, PCMs can regulate battery temperature without requiring additional power. However, their low thermal conductivity (approximately 0.2–0.4 W/mK) restricts heat dissipation and may lead to localized temperature rise in lithium-ion batteries. To improve the cooling performance, metallic fins have been incorporated into the PCM to enhance heat transfer and temperature uniformity.

Lv et al. [5] experimentally developed a composite PCM for lithium-ion BTMS. The incorporation of low-profile fins further enhanced heat dissipation and improved the cooling performance compared with the PCM-only configuration. Karimi et al. [6] experimentally compared metal-matrix and nanoparticle-enhanced PCM composites for cylindrical lithium-ion battery cooling. The study identified the metal-matrix PCM as the most effective approach for improving thermal management among the investigated composites.

Several numerical studies have examined the effect of fin geometry on battery cooling performance. Sun et al. [7] proposed a composite thermal management system incorporating PCM, aluminium fins, and graphite sheets for cylindrical lithium-ion batteries. It was demonstrated that the combined enhancement effectively improved heat dissipation by overcoming the low thermal conductivity of conventional PCM. Chen et al. [8] numerically investigated extended surfaces embedded in paraffin PCM for cooling cylindrical lithium-ion batteries. The optimum fin configuration reduced the maximum battery temperature and enhanced PCM melting performance. Mansir et al. [9]

numerically evaluated triangular fins in a PCM-based BTMS for cylindrical lithium-ion batteries. The results showed that fin dimensions influenced heat transfer, PCM melting behaviour, and battery temperature. Wider fins provided better thermal control than narrower fins. Zhang et al. [10] proposed nine branch-fin designs based on a conventional straight fin for a PCM-based BTMS. The optimal branch-fin configuration improved heat transfer, extended battery operating time, and reduced the system weight while maintaining the same system volume.

Recent studies have investigated novel fin configurations to improve the performance of PCM-based BTMS. Liu et al. [11] proposed a PCM-based BTMS incorporating spiral fins for cylindrical lithium-ion batteries. Compared with conventional circular fins, the spiral fin design reduced battery temperature and improved temperature uniformity. Choudhari et al. [12] numerically investigated the combined effects of fin geometry, fin number, PCM thickness, discharge rate, and heat transfer coefficient on the thermal performance of a PCM-based BTMS. Based on parametric analysis, the authors proposed an optimized battery module for enhanced thermal management.

Recent studies have explored advanced PCM-based BTMS designs to further enhance battery thermal management. Zare et al. [13] proposed a PCM-based BTMS incorporating internal and external fins for cylindrical lithium-ion batteries. The optimum fin configuration provided superior thermal performance and a more uniform cooling effect than the system without fins. Hussien et al. [14] proposed a PCM-based BTMS with a novel conical cylindrical chamber, significantly reducing the peak battery temperature and enhancing passive cooling performance. Heyhat et al. [15] investigated the influence of fins, metal foam, and nanoparticles on the thermal performance of a PCM-based BTMS for an 18650 Li-ion battery. The fin-enhanced PCM configuration reduced the average battery temperature by approximately 2–4 K compared with pure PCM. Srivastava et al. [16] experimentally and numerically investigated the effects of PCM type, PCM thickness, charging/discharging rate, and ambient temperature on battery thermal performance. The PCM reduced battery surface temperature, with Eicosane exhibiting the best cooling performance.

Although previous studies have demonstrated the effectiveness of PCM-based BTMS incorporating fins, most investigations have primarily focused on single-material fins, such as aluminium or copper, and the optimization of fin geometry, fin number, and PCM thickness. Systematic studies on Cu-Al bimetallic fin configurations for PCM-based cooling of cylindrical lithium-ion batteries remain limited. Therefore, the present study investigates the thermal performance of a PCM-assisted BTMS employing Cu-Al bimetallic fins with varying material proportions and PCM thicknesses to identify an optimal configuration that balances thermal performance and structural mass.

2 Numerical Model and Methodology

2.1 Geometry and Physical Model

A passive battery thermal management system based on PCM and radial fins is considered to regulate the temperature of a cylindrical lithium-ion battery. The computational domain consists of a single 18650 lithium-ion cell surrounded by a PCM enclosure with four symmetrically arranged radial fins of 2 mm thickness, as illustrated in Fig. 1.

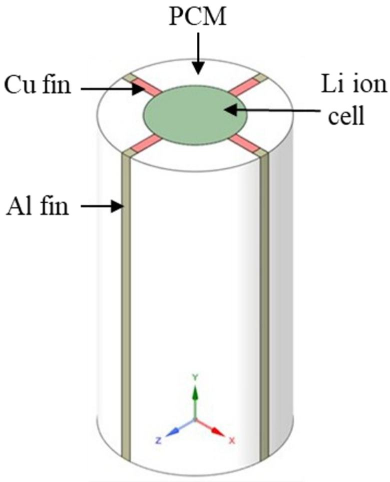

Fig. 1. 3D geometry of the cylindrical Li-ion battery with PCM and four radial fins.

The 18650 cell has a height of 65 mm and a diameter of 18 mm, which are typical dimensions for commercially available cylindrical lithium-ion batteries. The PCM domain surrounds the battery and acts as a thermal buffer by absorbing heat generated during battery discharge through latent heat storage. However, the low thermal conductivity of most PCMs limits heat transfer within the storage medium. To enhance heat dissipation, metallic fins are incorporated between the battery surface and the PCM to facilitate heat spreading and accelerate the melting process. In the present study, four radial fins are attached to the battery surface and extend into the PCM region. The fin thickness is fixed at 2 mm, while the PCM thickness surrounding the battery is varied as 4 mm, 8 mm, and 12 mm to evaluate the effect of PCM volume on the thermal performance of the battery thermal management system. The fins are modelled as Cu-Al bimetallic structures, and different copper–aluminium proportions are considered to examine the thermal-mass trade-off associated with the fin material composition as shown in Fig. 2. In the present work, RT-42 paraffin is chosen as PCM material. The solidus temperature and liquidus temperature of PCM is 311.15 K and 316.15 K [12].

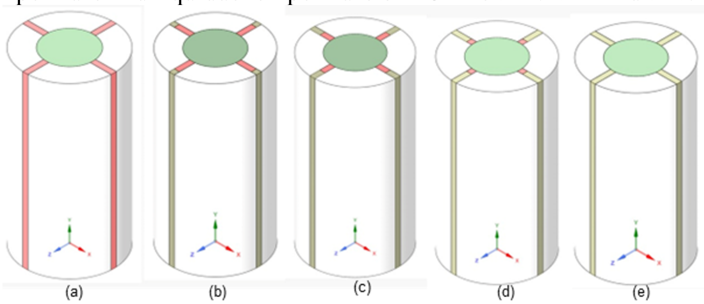

Fig. 2. Geometrical model showing different fin material proportions (a) 100Cu, (b) 75Cu-25Al, (c) 50Cu-50Al, (d) 25Cu-75Al, (e) 100Al

2.2 Governing Equations

The transient heat transfer and phase change processes in the PCM-based battery thermal management system are governed by the conservation equations of mass, momentum, and energy [12].

The continuity equation for incompressible flow is expressed as:

$$\nabla \cdot \vec{V} = 0 \quad (1)$$

The momentum equation governing fluid motion in the PCM region is given by:

$$\rho\left(\frac{\partial \vec{V}}{\partial t} + \vec{V} \cdot \nabla\vec{V}\right) = -\nabla p + \mu\nabla^2\vec{V} + \vec{S} \quad (2)$$

where ρ is the density, $\vec{V}$ is the velocity vector, p is pressure, μ is dynamic viscosity, and $\vec{S}$ represents the momentum source term used in the phase change modelling.

The energy equation governing heat transfer in the battery, fins, and PCM domains is expressed as:

$$\rho c_p \frac{\partial T}{\partial t} = \nabla \cdot (k\nabla T) + \dot{Q} \quad (3)$$

where c_p is specific heat capacity, k is thermal conductivity, T is temperature, and $\dot{Q}$ represents the volumetric heat generation within the battery.

The phase change process of the PCM is simulated using the enthalpy–porosity method, in which the liquid fraction of PCM varies between zero (solid) and one (fully melted). The mushy zone is treated as a porous medium, and the momentum source term is used to suppress velocity in the solid PCM region [17].

To simplify the numerical analysis while capturing the essential thermal behaviour of the battery-PCM system, following assumptions are considered. The thermophysical properties of the battery, PCM, and fin materials are assumed to remain constant during the simulation, except for the PCM during the phase change process. Heat generation within the battery is considered uniform and corresponds to the specified discharge rate. Perfect thermal contact is assumed between the battery, fins, and PCM, neglecting any interfacial thermal resistance. Heat transfer within the battery and fins occurs primarily through conduction, while both conduction and natural convection are considered in PCM during melting. Radiation heat transfer is neglected due to its relatively small contribution compared to conduction and convection. Table 1 shows the thermophysical properties of Li-ion cell, PCM, fins (aluminium and copper), and acrylic cover.

Table 1. Thermophysical properties of Li-ion cell, Paraffin, Acrylic, Aluminium, Copper

Material	**Density (kg/m^3)**	**Specific heat capacity (J/kg K)**	**Thermal conductivity (W/m K)**	**Dynamic viscosity (kg/ms)**	**Thermal expansion coefficient (1/K)**

Li-ion cell [12]	2720	300	3	-	-
Paraffin (RT-42) [12]	820	2000	0.2	0.02	1.0×10^{-4}
Aluminium [17]	2719	871	202.4	-	-
Copper [17]	8978	381	387.6	-	-
Acrylic [12]	1215	1300	0.17	-	-

2.3 Boundary conditions

The thermal boundary conditions applied in the numerical model are defined based on the operating conditions of the battery and the surrounding cooling environment.

Battery cell. During operation, the lithium-ion battery generates heat due to internal electrochemical reactions and ohmic losses. In the present study, the heat generation within the battery is represented as a uniform volumetric heat source corresponding to a 2C discharge rate (41,788 W/m^3) [12]. This assumption is widely adopted in numerical studies of battery thermal behaviour and allows the thermal response of the cooling system to be evaluated effectively.

Battery-PCM interface. At the interface between the battery surface, surrounding PCM and fins, perfect thermal contact is assumed. This implies that the thermal resistance at the interface is negligible and heat transfer occurs through conduction from the battery surface directly into the PCM and the attached fins.

Outer surface of PCM enclosure. The outer boundary of the PCM domain is exposed to the surrounding environment. Heat dissipation from this surface is modelled using a convective boundary condition to represent natural cooling by ambient air. The convective heat transfer coefficient is taken as 5 W/m^{2}K.

Ambient condition. Initially, the entire computational domain, including the battery, PCM, and fins, is assumed to be at a uniform ambient temperature before the battery begins to discharge. This initial condition ensures that the subsequent temperature rise and PCM melting behaviour are solely due to the heat generated by the battery during operation.

2.4 Model validation and grid independent study

Model validation was performed by comparing the present numerical results with the study reported by Choudhari et al. [12]. The average temperature of the Li-ion cell at a 3C discharge rate was considered for the comparison. As shown in Fig. 3, the temporal variation of the average cell temperature predicted in the present study follows the same trend as the results reported in Choudhari et al. [12]. The deviation between the two was within ±2% indicating good agreement and confirming the reliability of the numerical model.

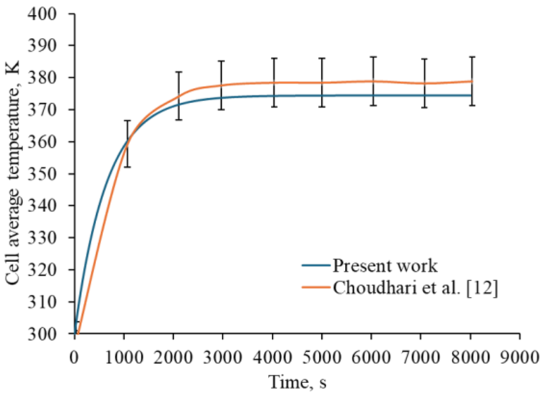

Fig. 3. Model validation with Choudhari et al. [12]

A grid independent study was conducted to ensure that the numerical solution is independent of mesh resolution. Four meshes with element sizes of 1.5 mm, 1.34 mm, 1.2 mm, and 0.9 mm, corresponding to 30,149; 47,200; 61,790, and 95,980 elements, respectively, were studied. The analysis was performed for a representative case of 75Cu-25Al with four fins, operating at a 2C discharge rate and with an external heat transfer coefficient of 5 W/m^2K. The predicted average cell temperature was used as the evaluation parameter. The results showed that the temperature variation decreased with mesh refinement and became nearly constant for the finer meshes. The difference between the two finest meshes was relatively small, indicating that further refinement had negligible influence on the solution. Therefore, the mesh containing 95,980 elements was selected for all subsequent simulations.

3 Results and Discussion

This section presents the thermal behaviour of the PCM-based battery thermal management system under a 2C discharge rate with four fins and an external convective heat transfer coefficient of 5 W/m^2K. The analysis focuses on two key design parameters: PCM thickness and fin material composition. Initially, temperature and liquid fraction contours at t = 400 s and t = 2000 s are examined to illustrate the heat transfer and PCM melting characteristics during the early and intermediate stages of the discharge process. Subsequently, the influence of PCM thickness on the thermal response of the system is analysed, followed by the effect of different Cu-Al fin compositions on battery cooling performance. The PCM melting behaviour is further evaluated using the liquid fraction at the post-discharge stage (t = 8000 s) to assess the overall PCM utilization. Finally, the results are interpreted from a thermal-mass trade-off perspective to identify bimetallic fin configurations that provide effective thermal management while reducing copper usage.

3.1 Temperature Distribution and PCM Melting Characteristics

Figure 4 presents the temperature contours in the PCM domain surrounding the cylindrical battery cell at two representative time instants during the discharge process. At the initial stages of operation, heat generated by the battery is conducted through the radial fins into the surrounding PCM, resulting in a gradual temperature rise near the battery–PCM interface.

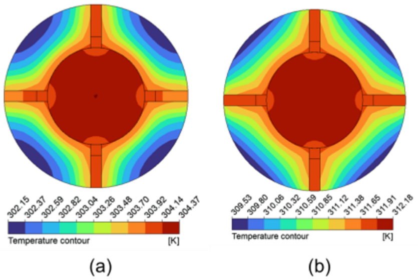

Fig. 4. Temperature contours of PCM for the representative case (25Cu–75Al fins, 8 mm PCM) at (a) 400 s and (b) 2000 s.

As shown in the contours, the highest temperature region is concentrated around the battery surface, where heat generation occurs. The radial fins effectively conduct heat away from the battery surface and distribute it into the PCM domain, forming distinct thermal pathways along the fin directions. This leads to a relatively symmetric temperature distribution around the battery cell, indicating effective heat spreading through the fins. As time progresses, the temperature field expands radially outward from the battery towards the PCM enclosure. The PCM region near the battery and fins experiences a higher temperature rise, which initiates the melting process. In contrast, the outer PCM regions remain at lower temperatures due to the limited heat penetration at early stages. The temperature gradients observed between the battery surface and the outer PCM boundary highlight the role of fins in enhancing radial heat conduction and promoting PCM activation. Overall, the temperature contours demonstrate that the fins facilitate efficient heat transfer from the battery to the PCM, enabling gradual thermal energy distribution within the PCM domain and initiating the phase change process.

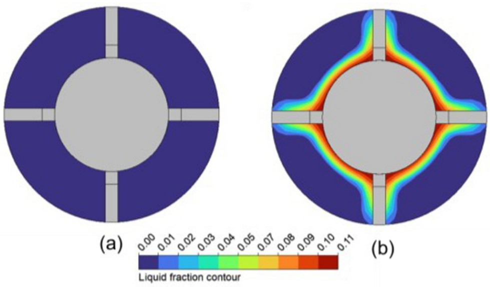

Fig. 5. Liquid fraction contours of PCM for the representative case (25Cu–75Al fins, 8 mm PCM) at (a) 400 s and (b) 2000 s.

Figure 5 presents the liquid fraction contours of the PCM surrounding the battery for the representative configuration with 25Cu-75Al fins and 8 mm PCM thickness at (a) t = 400 s and (b) t = 2000 s. At t = 400 s, the PCM remains completely solid, as indicated by a liquid fraction value of zero throughout the PCM domain. This suggests that the temperature rise in the early stage of discharge is insufficient to initiate phase change. As the discharge progresses to t = 2000 s, partial melting begins near the battery-PCM interface where the temperature is relatively higher due to heat generation within the battery. The presence of fins enhances heat conduction from the battery into the PCM region, resulting in localized melting along the fin directions. Consequently, higher liquid fraction regions are observed adjacent to the fins and around the battery surface, while the outer PCM region remains largely solid. These contours indicate that the fins play a significant role in promoting heat spreading within the PCM and facilitating the initial stage of PCM activation.

3.2 Effect of PCM Thickness on Thermal Response

Figure 6 illustrates the temporal variation of average cell temperature and PCM liquid fraction for different PCM thicknesses (4 mm, 8 mm, and 12 mm). Increasing PCM thickness reduces the rate of temperature rise due to the larger latent heat storage capacity available for heat absorption. The 12 mm PCM configuration exhibits the lowest temperature increase throughout the discharge process, indicating improved thermal buffering. However, the melting rate decreases with increasing PCM thickness, as reflected by the slower liquid fraction evolution for thicker PCM layers. This behaviour is attributed to the larger PCM volume that requires greater energy for complete melting. These results indicate that while increasing PCM thickness enhances temperature regulation, the improvement becomes less pronounced beyond moderate PCM thicknesses.

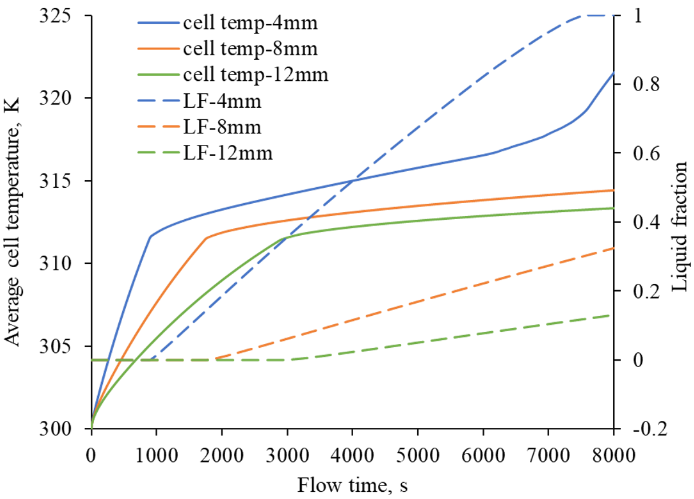

Fig. 6. Evolution of average cell temperature and PCM liquid fraction for different PCM thicknesses.

3.3 Effect of Fin Material Composition

The influence of fin material composition on the thermal behaviour of the battery module is analysed by varying the copper-aluminium proportion in the fins while keeping other parameters constant (four fins, fin thickness of 2 mm, and convection coefficient of 5 W/m^{2}K). Figure 7 shows the temporal variation of PCM liquid fraction for different fin material compositions.

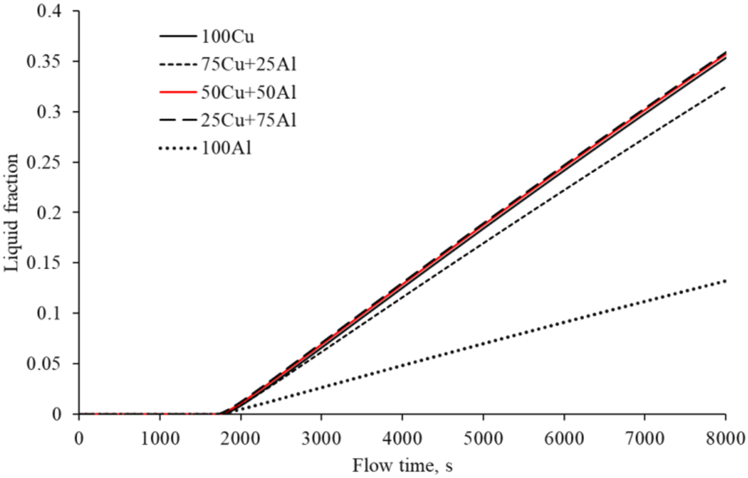

Fig. 7. Evolution of PCM liquid fraction for different fin material compositions.

PCM melting begins at approximately 1800-2000 s, corresponding to the time at which the PCM temperature reaches its melting range. After this stage, the liquid fraction increases progressively as the PCM absorbs heat generated by the battery. The results indicate that fins containing copper significantly enhance PCM melting compared with the aluminium-only case. The 100Al configuration exhibits the lowest liquid fraction, reaching only about 0.13 at 8000 s, due to the lower thermal conductivity of aluminium which limits heat spreading into the PCM domain.

In contrast, the bimetallic configurations (25Cu-75Al and 50Cu-50Al) exhibit the highest PCM melting behaviour, reaching liquid fractions of approximately 0.36 at 8000 s. These configurations provide improved heat spreading from the battery surface while still allowing localized temperature rise that promotes effective PCM melting. Increasing the copper proportion beyond this level does not significantly enhance PCM activation. The 75Cu-25Al and 100Cu cases show similar melting trends, indicating that once sufficient heat conduction is achieved, further increases in fin conductivity produce limited additional benefit.

Overall, the results demonstrate that intermediate Cu-Al compositions provide effective PCM activation while avoiding excessive copper usage, suggesting that bimetallic fins can deliver thermal performance comparable to copper fins with reduced material mass.

3.4 PCM Melting Behaviour and Thermal Mass Trade-off

The influence of fin material proportion on PCM melting behaviour was evaluated by comparing the liquid fraction at t = 8000 s, as shown in Fig. 8. The results indicate that the PCM liquid fraction increases with increasing copper content in the fins due to the higher thermal conductivity of copper, which enhances heat transfer from the battery surface to the surrounding PCM. For the 100Al configuration, the PCM liquid fraction is relatively low (≈ 0.13), indicating limited heat propagation into the PCM. Introducing copper into the fin structure significantly improves the melting behaviour. The 25Cu-75Al and 50Cu-50Al bimetallic configurations show a considerable increase in liquid fraction, demonstrating enhanced heat spreading capability. Further increasing the copper proportion to 75Cu-25Al results in a liquid fraction of ≈ 0.32, which is very close to the value obtained for the pure copper fins (≈ 0.35). These results suggest that bimetallic fin configurations can achieve PCM melting behaviour comparable to pure copper fins while reducing the overall copper content. This highlights the potential of Cu-Al bimetallic fins in achieving efficient thermal management with reduced material usage.

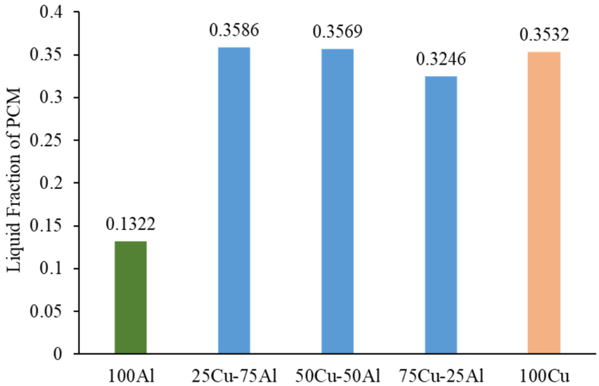

Fig. 8. Liquid fraction of PCM at t = 8000 s for different fin material compositions (4 fins, 2C discharge rate, h = 5 W/m^2K)

Although increasing copper content generally enhances the thermal conductivity of the fins, the PCM melting behaviour does not increase strictly monotonically with copper proportion. As shown in Fig. 8, the introduction of copper into the fin structure significantly enhances PCM activation compared with the pure aluminium case. The 25Cu-75Al and 50Cu-50Al configurations exhibit the highest liquid fraction values (≈0.36), indicating effective heat spreading from the battery to the PCM. A slight reduction in liquid fraction is observed for the 75Cu-25Al configuration (0.3246), which may be attributed to localized heat transfer near the fin-battery interface during the transient melting process. The pure copper configuration again shows a relatively high liquid fraction (≈0.35). Overall, the results indicate that bimetallic fin configurations can achieve PCM melting behaviour comparable to pure copper fins while reducing copper usage. Although pure copper fins provide slightly higher PCM melting, the associated increase in fin mass is significant. Bimetallic configurations therefore provide a favourable balance between thermal performance and material usage.

4 Conclusion

This study numerically investigated the influence of fin material composition and PCM thickness on the thermal performance of a PCM-based battery thermal management system for a cylindrical Li-ion cell under 2C discharge. The results show that radial fins effectively enhance heat spreading from the battery surface to the PCM, initiating the melting process and moderating temperature rise. Increasing PCM thickness improves the thermal buffering capability of the system; however, the rate of PCM melting decreases due to the larger latent heat capacity. The analysis of fin material composition indicates that Cu-Al bimetallic fins provide comparable PCM activation to pure copper fins while reducing the use of high-density copper. In particular, intermediate configurations such as 25Cu-75Al and 50Cu-50Al demonstrate enhanced melting behaviour relative to pure aluminium fins with significantly lower material mass than pure copper fins. These results suggest that fin material distribution can serve as an effective design parameter to balance thermal performance and structural mass in PCM based BTMS.

References

1. International Energy Agency: *World Energy Outlook 2023*. IEA Publications, Paris (2023)
2. Our World in Data: CO_2 emissions from transport. Global Carbon Project dataset (2024)
3. U.S. Department of Energy: Where the Energy Goes: Electric Cars. FuelEconomy.gov, Office of Energy Efficiency and Renewable Energy (2024).
4. International Energy Agency: *Global EV Outlook 2024*. IEA Publications, Paris (2024)
5. Lv, Y., Yang, X., Li, X., Zhang, G., Wang, Z., Yang, C.: Experimental study on a novel battery thermal management technology based on low density polyethylene-enhanced composite phase change materials coupled with low fins. *Applied Energy* **178**, 376–382 (2016). https://doi.org/10.1016/j.apenergy.2016.06.058.
6. Karimi, G., Azizi, M., Babapoor, A.: Experimental study of cylindrical lithium-ion battery thermal management using phase change materials. *J. Energy Storage* **8**, 168–174 (2016). https://doi.org/10.1016/j.est.2016.08.005.
7. Sun, Z., Fan, R., Yan, F., Zhou, T., Zheng, N.: Thermal management of the lithium-ion battery by the composite PCM-Fin structures. *Int. J. Heat Mass Transfer* **145**, 118739 (2019). https://doi.org/10.1016/j.ijheatmasstransfer.2019.118739.
8. Chen, H., Abidi, A., Hussein, A. K., Younis, O., Degani, M., Heidarshenas, B.: Investigation of the use of extended surfaces in paraffin wax phase change material in thermal management of a cylindrical lithium-ion battery: Applicable in the aerospace industry. *J. Energy Storage* **45**, 103685 (2022). https://doi.org/10.1016/j.est.2021.103685.
9. Mansir, I.B., Sinaga, N., Farouk, N., Aljaghtham, M., Diyoke, C., Nguyen, D.D. Numerical simulation of dimensions and arrangement of triangular fins mounted on cylindrical lithium-ion batteries in passive thermal management. *J. of Energy Storage*, **50**, 104392 (2022). https://doi.org/10.1016/j.est.2022.104392.

10. Zhang, F., Lu, F., Liang, B., Zhu, Y., Gou, H., Xiao, K., He, Y.: Thermal performance analysis of a new type of branch-fin enhanced battery thermal management PCM module. *Renew. Energy* **206**, 1049-1063 (2023). https://doi.org/10.1016/j.renene.2023.02.083.
11. Liu, J., Ma, Q., Li, X.: Numerical simulation of spiral fins combined with PCM for cylindrical lithium-ion battery thermal management. *Energies* **15(23)**, 8847 (2022). https://doi.org/10.3390/en15238847.
12. Choudhari, V.G., Dhoble, A.S., Panchal, S.: Numerical analysis of different fin structures in phase change material module for battery thermal management system and its optimization. *Int. J. Heat Mass Transfer* **163**, 120434 (2020). https://doi.org/10.1016/j.ijheatmasstransfer.2020.120434.
13. Zare, P., Perera, N., Lahr, J., Hasan, R.: A novel thermal management system for cylindrical lithium-ion batteries using internal-external fin-enhanced phase change material. *Appl. Therm. Eng.* **238**, 121985 (2024). https://doi.org/10.1016/j.applthermaleng.2023.121985.
14. Hussien, S.A., Ali, A.B., Alkhatib, O.J., Mahariq, I.: Enhanced passive thermal management of lithium-ion batteries with conical cylindrical chamber incorporating various phase change materials. *Sci. Rep.* **15(1)**, 35675 (2025). https://doi.org/10.1038/s41598-025-19597-0.
15. Heyhat, M.M., Mousavi, S., Siavashi, M.: Battery thermal management with thermal energy storage composites of PCM, metal foam, fin and nanoparticle. *J. Energy Storage* **28,** 101235 (2020). https://doi.org/10.1016/j.est.2020.101235.
16. Srivastava, G., Nandan, R., Das, M.: Thermal runaway management of Li ion battery using PCM: A parametric study. *Energy Convers. Manag. X* **16,** 100306 (2022). https://doi.org/10.1016/j.ecmx.2022.100306.
17. ANSYS Inc.: *ANSYS Fluent User's Guide, Release 2025 R2*. ANSYS Inc., Canonsburg, PA (2025).